
Research article

Signal transduction from ligand-receptor binding associated with the formation of invadopodia in an invasive cancer cell

Noorehan Yaacob^{1,*}, Sharidan Shafie¹, Takashi Suzuki² and Mohd Ariff Admon¹

¹ Department of Mathematical Sciences, Faculty of Science, Universiti Teknologi Malaysia, Skudai, 81310 Johor Bahru, Johor, Malaysia

² Center for Mathematical Modeling and Data Science, Osaka University, Japan

* Correspondence: Email: noorehanyaacob@gmail.com.

Abstract: Invadopodia are finger-like protrusions that are commonly spotted at the membrane of the invasive cancer cell. These structures are a major cause of death among cancer patients through metastasis process. Signal transduction stimulated upon contact between ligand and membrane receptors is identified as one of key factors in invadopodia formation. In this study, a time-dependent mathematical model of signal and ligand is investigated numerically. The moving boundary of plasma membrane is taken as a zero-level set function and is moved by the velocity that accounted as the difference of gradient between intra-cellular signal and extra-cellular ligand. The model is solved using a combination of ghost with linear extrapolation and finite difference methods. The results showed that the stimulation of signal from membrane associated ligand consequently moved the plasma membrane outward as time increases. The highest densities of signal and ligand are recorded on the membrane and slowly diffused into intra-cellular and extra-cellular regions, respectively.

Keywords: ghost fluid method; invadopodia; level set method; ligand; protrusion; signal transduction

1. Introduction

As stated in [1], the development of cancer cells is caused by the malignant transformation. The occurrence of cancer commences due to the uncontrolled proliferation of the cancer cells and the inactivation of the tumor suppressor pathways [2]. Also, genetic instability will cause the cell to proliferate and leading to the formation of tumors. Generally, the aspects that can contribute to the formation of cancer are the self-sufficiency in proliferative signaling, evasion of tumor growth suppressors, apoptosis, invasion of tissue, angiogenesis, and metastasis [3]. The invasive cancer cell can invade the other tissue and thus lead to the occurrence of the metastasis process. Metastasis is the dissemination of tumors from the primary location to other parts of the body and this is a concerning issue because the secondary tumor is more threatening and can contribute to the high death cases among cancer patients [4,5].

In order for cancer to spread, the metastatic cancer cells have to penetrate several physical barriers to escape from the primary tumor [6,7]. For that purpose, finger-like protrusions, or invadopodia are formed and enable the invasive cancer cells to pass through it. According to [8], invadopodia are obtained from the stimulation of a signal that makes a branched actin assembly at the sites of the membrane. The formation of invadopodia involves several biological processes and it can be observed on the plasma membrane. A series of studies from [9–13] have widely explored the cancer cell invasion at the tissue level. In their study, they have included many factors that can support the cancer cell invasion in tissue through the explanation of mathematical modeling.

Meanwhile, invadopodia can be observed in the sub-cellular region. Therefore, in recent years, the sub-cellular part has been the focus of study. According to [14–16], the formation of invadopodia begins with the degradation of the extra-cellular matrix (ECM) by the matrix-degrading enzymes (MDEs) such as matrix metalloproteinases (MMPs). After the degradation of ECM, the ligand is produced and diffused to the extra-cellular region. The signal is stimulated on the intra-cellular region after the binding of the ligand with the membrane-associated membrane such as epidermal growth factor receptor (EGFR) has occurred. The stimulation of the signal caused the up-regulation of the MMPs and actin polymerization.

The formation of invadopodia from the perspective of mathematical modeling has been proposed by [14]. They have been introduced the mathematical modeling for the formation of invadopodia through modeling the equations for ECM, MMPs, ligand, and actin. The positive feedback loop on the invadopodia formation has been shown in this study. In their study, they managed to show the level of invasiveness through the different rates of MMPs. Since they are implemented on the fixed boundary domain, there is an issue raised when actin is spotted at the extra-cellular region, and it contradicts the biological fact that actin is in the intra-cellular region.

In the meantime, [15,17] suggested a new variable in the formation of invadopodia, which is signal transduction. Mathematical modeling is performed on one-dimensional time-dependent signal transduction. Also, these studies highlighted the movement of the free boundary interface (plasma membrane) to indicate the formation of protrusions on the interface by using the formula of the gradient of intra-cellular signal. Their study successfully displayed the changes in the location of the membrane as time increases. Also, the concentration of the signal can be indicated as higher on the plasma membrane. Additionally, a study on the formation of invadopodia that emphasized signal transduction has been considered by [18]. The two-dimensional time-independent signal transduction is studied, and from this approach, it is obvious that outward

protrusions or invadopodia existed on the plasma membrane.

Besides, [16,19,20] explained the formation of protrusions on the interface by highlighting the mathematical model of two-dimensional ligand and signal. They also mentioned the method of the level set to solve the free boundary interface. Those studies have applied the method of ghost fluid with linear extrapolation and second-order centered difference to discretize the neighboring and regular grid points, respectively. In the meantime, the polymerization of actin is accounted for by the gradient of the intra-cellular signal and this consequently moves the plasma membrane. Apart from that, the concentration of MMPs is set as a Gaussian function on the interface. Further, [21] has studied the two-dimensional time-independent of signal and ligand with the Dirichlet boundary condition for both signal and ligand regions.

Hence, by considering the above-mentioned studies, this paper explored the two-dimensional time-dependent signal transduction and ligand for the formation of invadopodia. This is the new mathematical modeling proposed since models with time constraints have not yet been implemented. Meanwhile, the displacement of the interface is accounted for as jump velocity and this is a new technique to deal with the velocity on the interface. Also, the level set method is presented to capture the movement of the interface by locating the interface as the zero-level set function. Other methods that are involved in the numerical computation are second-order centered difference and ghost fluid with linear extrapolation particularly to solve for the regular and neighboring grid points, respectively.

2. The mathematical modeling

2.1. The equations of the mathematical modeling

In this section, the mathematical modeling for the formation of invadopodia on the plasma membrane of an individual cancer cell is described. There are four key variables focused on this paper to interpret the molecular interactions between ligand denoted by $c^*(\mathbf{x}, t)$, signal denoted by $\sigma(\mathbf{x}, t)$, the velocity or the movement of the free boundary interface denoted by $\mathbf{v}(\mathbf{x}, t)$, and the velocity extension denoted by $\mathbf{w}(\mathbf{x}, t)$. In this paper, the actin polymerization is accounted as the difference of gradient between the intra-cellular signal and extra-cellular ligand that consequently moves the interface. The molecular interactions between the variables are described in the square domain as in Figure 1a and defined as $\Omega = \Omega_t^{c^*} \cup \Gamma_t \cup \Omega_t^\sigma$ to represent the extra-cellular, interface, and intra-cellular regions, respectively. Also, Figure 1b portrayed the schematic diagram for the process of formation of invadopodia in terms of biological.

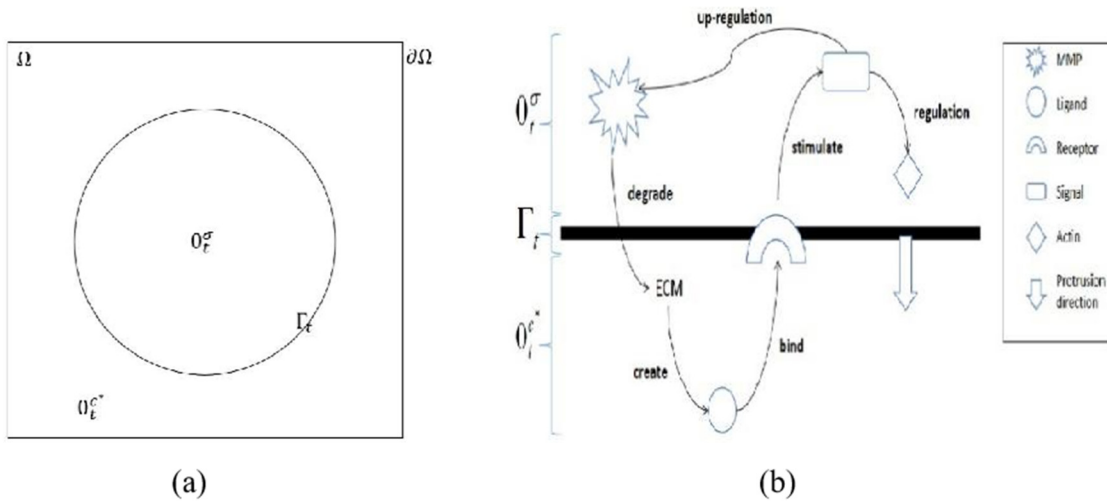


Figure 1. The figures showed the geometrical setting for the complete domain in two-dimensional invadopodia formation and the biological flow for the process of invadopodia formation. The existence of MMPs on the plasma membrane led to the degradation of ECM. After the degradation activity, the ligand is created and diffused to the extra-cellular region. Ligand is bound with the membrane-associated receptor, EGFR, and the signal is stimulated in the intra-cellular region. The signal will initiate the up regulation of MMPs and polymerization of actin. Also, the movement of the interface is explained as the difference in a gradient of intra-cellular signal and extra-cellular ligand (a) The geometrical setting for the complete domain of two-dimensional invadopodia formation and (b) The schematic diagram for the process of formation of invadopodia.

This work is carried out after considering the gap from the work in Gallinato et al. where the time-dependent (parabolic equation) model has been considered. By considering the time-dependent model, the simulation can be carried out for a longer time. However, the elliptic model proposed by Gallinato et al is reasonable for a short time only because of the time is approaching zero. Thus, the parabolic version is carried out to investigate the behaviors of the protrusions as time increases. In addition, referring to the model in Gallinato et al., the Neumann condition has been applied for ligand (c^*), however, this work emphasized the Dirichlet condition where on the interface, the concentration of a ligand is similar to the signal. In addition, the velocity is accounted for as the difference of gradient between intracellular signal and an extracellular ligand that is yet considered in Gallinato et al.

Equation 1 shows the dynamics of ligand where the creation of ligand begins with the occurrence of ECM degradation and thus ligand may diffuse to the extra-cellular region. Also, there is no ligand on the square domain since ligand is produced on the plasma membrane assuming that the ligand does not reach the boundary of domain. The ECM degradation is executed by the activity of the MMPs. Given that at any time t , the interface carried the flux of MMPs and is taken as a trigonometric function $g(\mathbf{x})$. On the other hand, Eq 2 refers to the signal transduction where the binding of the ligand with the receptor on the plasma membrane, in particular, EGFR will stimulate the signal. The signal is pivotal for the formation of invadopodia and this is not mentioned in [14]. However, it is introduced in [15–17]. The signal will be diffused to the intra-cellular region and bring to the activities of up-regulation of MMPs and polymerization of actin.

Actin is known as the cytoskeletal protein in cells and its polymerization leads to changes in the interface location. Hence, actin polymerization is assumed as the velocity of the interface. In previous works, [16,17,21], the velocity is set as the gradient of intracellular signal only. In this work, velocity is accounted for as the difference of gradient between intra-cellular signal and extra-cellular ligand (refer to Eq 3). This purpose is newly discovered, and this approach is appropriate since the signal and ligand situated in two different areas are used. Employing the level set method, the velocity with the whole domain is also required. Thus, the velocity extension proposed by Gallinato et al. is applied in this work (refer to Eq 4).

From the above explanations, the mathematical modeling for the formation of invadopodia are stated in Eqs 1–4.

Ligand dynamics:

$$\begin{aligned} c_t^* &= \Delta c^*, \quad \mathbf{x} \in \Omega_t^{c^*}, \quad t \in [0, T], \\ c^* &= 0, \quad \mathbf{x} \in \partial\Omega, \quad t \in [0, T], \\ c^* &= g(\mathbf{x}), \quad \mathbf{x} \in \Gamma_t, \quad t \in [0, T]. \end{aligned} \quad (1)$$

The stimulation of signal transduction:

$$\begin{aligned} \sigma_t &= \Delta\sigma, \quad \mathbf{x} \in \Omega_t^\sigma, \quad t \in [0, T], \\ \sigma &= c^*, \quad \mathbf{x} \in \Gamma_t, \quad t \in [0, T]. \end{aligned} \quad (2)$$

Velocity of the interface:

$$\mathbf{v} = \nabla\sigma - \nabla c^*, \quad \mathbf{x} \in \Gamma_t, \quad t \in [0, T]. \quad (3)$$

Velocity extension:

$$\begin{aligned} (\nabla\psi \cdot \nabla)\mathbf{w} &= 0, \quad \mathbf{x} \in \Omega, \quad t \in [0, T], \\ \mathbf{w} &= \mathbf{v}, \quad \mathbf{x} \in \Gamma_t, \quad t \in [0, T]. \end{aligned} \quad (4)$$

where ψ is the level set function.

3. Results and numerical simulations

In this section, the numerical simulation results are presented. The mathematical modeling is carried out in a two-dimensional space dimension with time constraints. In the numerical computation, the domain, Ω is described in square domain with size dimension in x and y axes are set to $[-L, L] \times [-L, L]$. The number of lattice points in x and y axes is set to $(M_x, M_y) = (100, 100)$. The step size for x and y is taken as $h = \frac{L}{M}$, where M is the size of the matrix and the time step is k . In this paper, the individual invasive cancer cell is focused on. Thus, the first level set is assigned as the equation of circle, $\psi_{i,j}^0 = x_i^2 + y_j^2 - r^2$ with radius set to r . The circle obtained is to portray the plasma membrane of an invasive cancer cell.

The regions of interface, intra-cellular, and extra-cellular are differed using the approach of $\psi_{i,j}^n = 0$, $\psi_{i,j}^n < 0$, and $\psi_{i,j}^n > 0$. From this procedure, the activities of signal and ligand can be distinguished. From the perspective of biology, the formation of invadopodia is a continuous process and it started from the degradation of the ECM by the MMPs. In this paper, the concentration of the

MMPs is cited in [16] and is presented as a function $g(\mathbf{x})$ where $g(\mathbf{x}) = \epsilon[2 + \cos(3\pi(x + y))\cos(\pi(x + 0.3))]$ and $\epsilon = 10^{-5}$. The parameter values used in the numerical computation are stated in Table 1. In this paper, the simulations are carried out in μm units. This is supported by the study in [29], where the inner diameter of many cancer cell lines is in μm units.

Table 1. List of parameter values.

Parameter	Values
L	1 μm
M	100 μm
r	$\frac{2}{3}\mu\text{m}$
k	$\frac{1}{3}\text{seconds}$

Meanwhile, the velocity extension is performed using the partial differential equations (PDEs) method to gain the information of the velocity from every area of the interface. Since the level set method is implemented, not only the velocity on the interface is needed, but the velocity of the whole domain is also essential. Thereafter, the level set function is updated using the equation of transport, $\psi_t + \mathbf{v} \cdot \nabla \psi = 0$ and the gradient of ψ is based on the second-order upwind scheme. Meantime, the velocity on the interface will be identical to the velocity extension or we will set it as $\mathbf{v} = \mathbf{w}$.

3.1. Initial results

Figure 2 are the initial distribution for the level set, ligand, and signal. First, the initial level set function is taken as the equation of a circle. As shown in Figure 2a, the circle in the square domain is to indicate the individual invasive cancer cell before the formation of invadopodia on the interface. Figures 2b,c are the initial distribution for ligand and signal. Suppose that the process is commencing only as MMPs degrade the ECM and in this case, the concentration of MMPs is assumed as a function g . Only then, the ligand and signal concentrations are received.

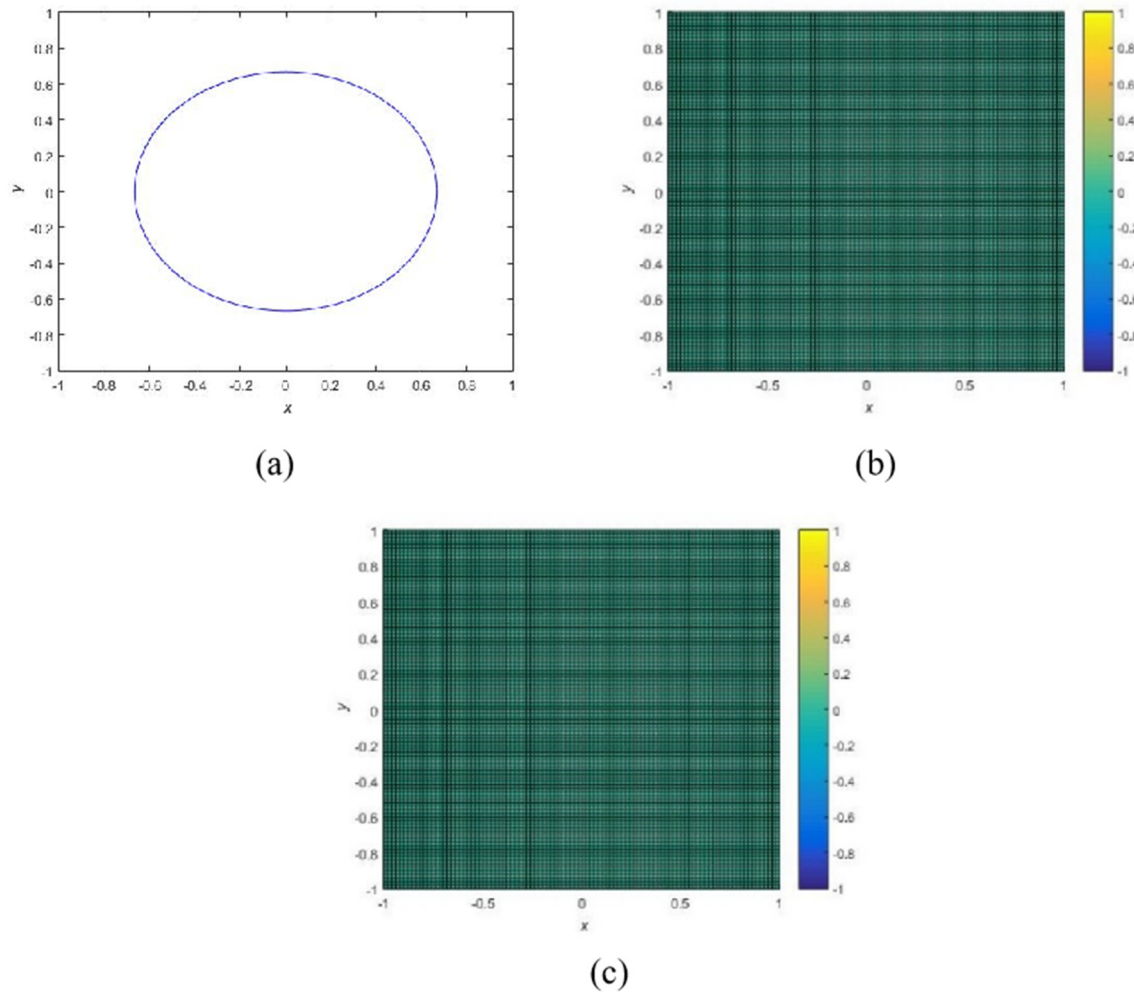


Figure 2. The distributions of (a) level set, (b) ligand, and (c) signal at $T = 0$ min.

3.2. After time steps

The numerical computation is continued until the protrusion on the interface is visible. At $T = 24$ min (478 iterations), small protrusions can be spotted at the interface as illustrated in Figure 3a. Also, the accumulation of ligand starts to begin particularly on the extra-cellular region as shown in Figure 3b. Apart from that, the stimulation of the signal can be observed in the intra-cellular region due to the ligand and receptor interactions. Referring to Figure 3c, there are some spots that can be noticed from the signal concentration. Pointing to the concentration of ligand and signal, the higher concentration is detected at the location of interface and this is proven from a study in [17] in which the concentration of signal is shown to be highest on the plasma membrane. This is also applicable to the concentration of ligand because, on the interface, the concentration of the ligand is similar to the concentration of signal. Hence, the activity on the intra-cellular and extra-cellular can be the reason for the invadopodia formation.

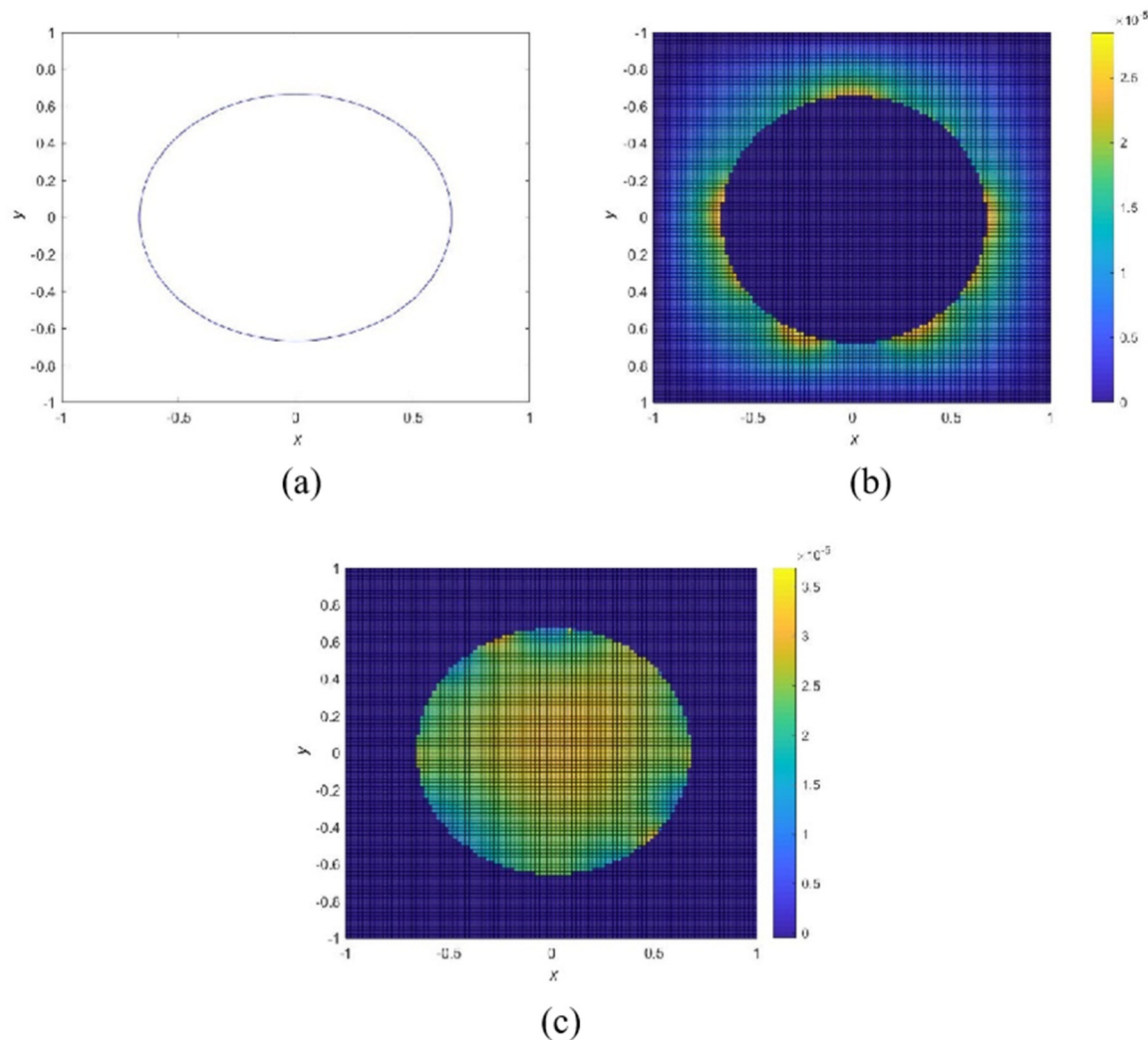


Figure 3. The distributions of (a) level set, (b) ligand, and (c) signal at $T = 24$ min (478 iterations).

By continuing the numerical computation, at $T = 35$ min (701 iterations), there are finger-like protrusion marks on the interface as illustrated in Figure 4a. Hence, the small protrusion at $T = 24$ min is observed to become longer as time proceeds. In medical terms, the appearance of this protrusion indicates that the cancer cell is becoming more invasive. Therefore, the movement of the cancer cell begins. Because the numerical computation is time-consuming, the computation is running up to 1000 iterations only. However, we believed that the protrusions would become longer as time increases. Referring to Figure 4b,c the distribution profiles of ligand and signal are similar to the location of protrusion. The protrusion can be spotted at the positive location of x and y axes. These figures also show that the signal is only existing in the intra-cellular region and ligand is in the extra-cellular region.

These outcomes successfully proved the interactions in the intra-cellular and extra-cellular regions to be similar in the biological study. Besides, with the aid of the jump velocity approach, the resulting protrusions accurately describe the real shape of the invadopodia which is the finger-like protrusions.

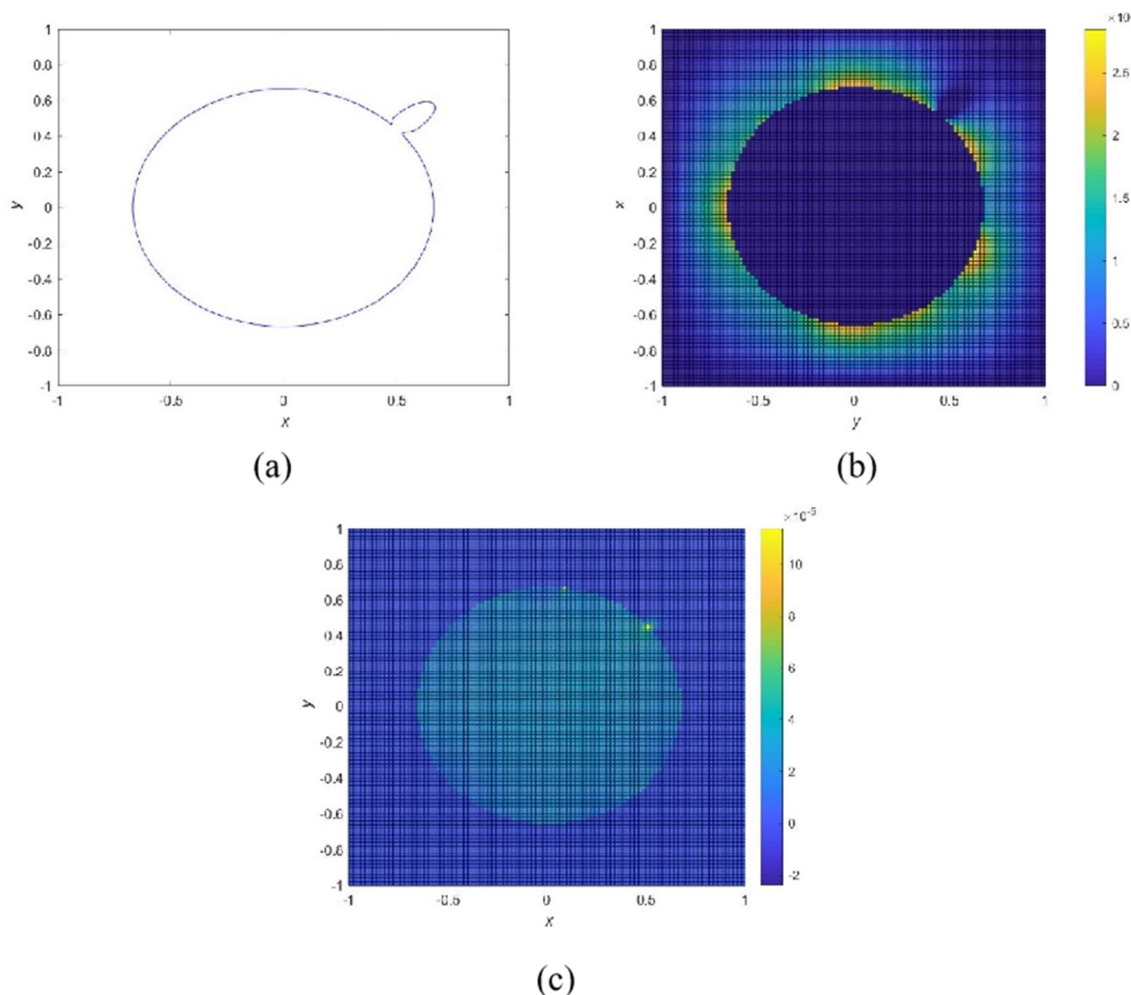


Figure 4. The distributions of (a) level set, (b) ligand, and (c) signal at $T=35$ min (701 iterations).

The cancer cells use invasive finger-like protrusions to degrade the ECM. According to [30], the presence of highly dynamic actin is likely to produce force for motility and longevity of the protrusions. Apart from that, the types of cortactin that initiate the actin polymerization has been explained in [31–33]. In our model, the invasive protrusion due to the force created by the actin polymerizations is accounted as jump velocity. Hence, the interface velocity by the actin moves the plasma membrane to the leading edge.

The signaling process by ligand-EGFR has been widely explored in [34,35] due to their prominent roles in cellular processes. It is a complex process and the signaling itself comprises various types of signaling such as autocrine, paracrine, and juxtacrine. Referring to the signaling process, it is only stimulated with the ligand-receptor interaction. Hence, the role of EGF or ligands has been described in [36,37]. Nevertheless, in our model, the behavior of ligand and signal to the dynamic of the invadopodia is investigated by taking the diffusion of ligand and signal to the extra-cellular and intra-cellular regions, respectively. As mentioned by [38], the appearance of adhesion signaling promotes the invadopodia formation. The signaling could enhance the invadopodia numbers due to the secondary effect of the increase in MMP proteinases activity. Therefore, from the simulations, the invadopodia are formed at the location of the high signaling process.

3.3. Numerical errors

In this section, the numerical errors are performed to verify the effectiveness of the numerical computation. In this paper, the numerical errors for the level set are focused and is given on Table 2 and in Figure 5. The formula used in getting the numerical errors is the maximum norm formula. The computation is carried out in a two-dimensional space with domain $[-1,1]^2$ discretized on a uniform grid. Due to time-consuming, the computation is conducted up to 1000 iterations ($T = 50$ min) and for every hundredth, the errors are observed. As shown in Table 2, the error is decreasing as iterations increased. The illustrated error is clearly seen in Figure 5.

Table 2. The numerical errors for the level set.

Iteration	Absolute error
100	0.0395999338
200	0.0387998713
300	0.0379998139
400	0.0371997622
500	0.0363997171
600	0.0355996797
700	0.0347996513
800	0.0339996339
900	0.0331996288
1000	0.0323996383

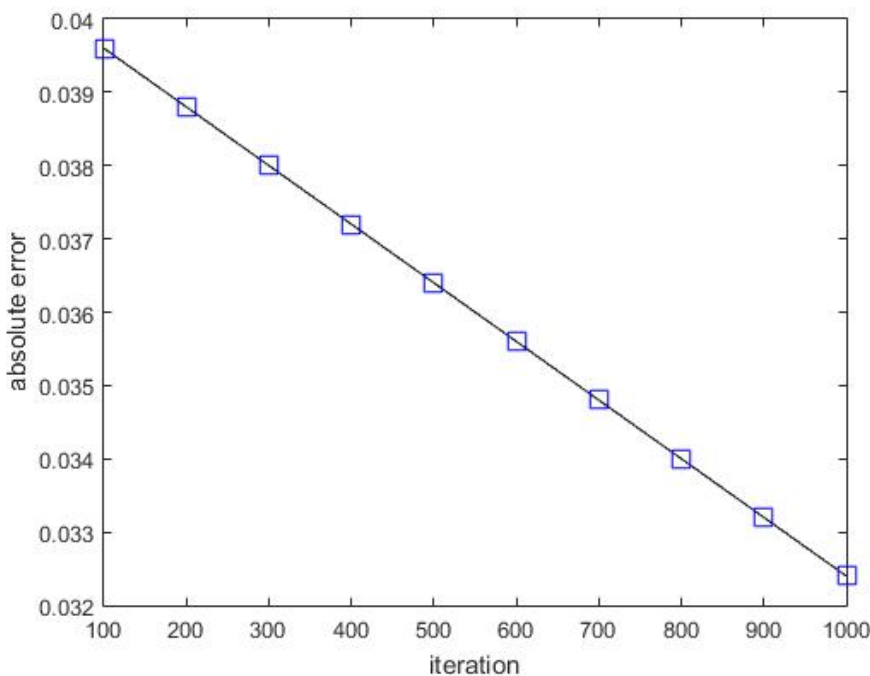


Figure 5. The numerical errors for the level set.

4. Conclusions

This paper studied the formation of finger-like protrusions or invadopodia on the plasma membrane of the invasive cancer cell. The mathematical modeling involved the PDEs model for signal, ligand, velocity, and velocity extension. In mathematical biology studies, [14] has explored the formation of invadopodia that comprises the densities of ligand, actin, ECM, and MMPs. Also, a new variable introduced by [15] which is a signal that is considered essential in the process of invadopodia formation. Additionally, the level set method is emphasized in this study to detect the interface location.

In this paper, the mathematical modeling of time-dependent signal and ligand is considered. Also, the polymerization of actin that consequently moves the interface is assumed as the velocity function and taken as the difference of gradient between intra-cellular signal and extra-cellular ligand. This is a new approach presented in this paper. Also, to obtain the velocity information from each area from the interface, the velocity extension is applied. The degradation of MMPs is also performed and taken as a function of g . The equations in the mathematical model are selected particularly to explain the biological interaction for the invadopodia formation.

In the numerical discretization scheme of the Laplace operator in signal and ligand, there exist types of points in the grid that should be considered, which are the points that are exactly on the interface, regular, and neighboring points. At the points that are exactly on the interface, the value is set as g , while regular and neighboring points are using second-order centered difference and ghost fluid with linear extrapolation, respectively. The level set method is also described to detect the location of the interface by setting the interface as the zero-level set function. The area of the interface, intra-cellular, and extra-cellular are can also be determined using this approach. The numerical results showed that the protrusion-like shape can be found on the interface, and it moves outward to represent the presence of the invadopodia. This result is relevant to show the cancer cell invasion process through metastasis at the sub-cellular level. The invadopodia expanded in size as time increased. In the meantime, the ligand and signal distribution also show high concentration at the place where the protrusion formed. This conveyed that, the protrusion can be spotted at the high level of ligand and signal densities. Also, referring to the signal and ligand distributions, it is indicated that the signal can be found on the intra-cellular region and ligand is on the extra-cellular region. Meanwhile, the numerical errors are also given to verify the effectiveness of the numerical computation.

Although the formation of invadopodia on the plasma membrane has been shown, the complete model on the formation of invadopodia is necessary to be executed. In future research, the mathematical model for the membrane-associated receptor, such as EGFR should be considered since it is one of the important factors that should be in the invadopodia formation. Also, the mathematical model for the signal and ligand can be improved by including the diffusive rate and decay term.

Acknowledgments

This research was partly supported by Ministry of Higher Education under Fundamental Research Grant Scheme (FRGS/1/2018/STG06/UTM/02/1) and Kementerian Pendidikan Tinggi Malaysia for the scholarship under the MybrainSC scheme.

Conflict of interest

The authors declare no conflict of interest.

References

1. Helfinger V and Schröder K (2018) Redox control in cancer development and progression. *Mol Aspects Med* 63: 88–98. <https://doi.org/10.1016/j.mam.2018.02.003>
2. Li B, Gordon GM, Du CH, et al. (2010) Specific killing of Rb mutant cancer cells by inactivating TSC2. *Cancer Cell* 17: 469–480. <https://doi.org/10.1016/j.ccr.2010.03.019>
3. Szabó A and Merks RMH (2013) Cellular potts modeling of tumor growth, tumor invasion, and tumor evolution. *Front Oncol* 3: 87 <https://doi.org/10.3389/fonc.2013.00087>
4. Franssen LC, Lorenzi T, Burgess AEF, et al. (2019) A mathematical framework for modelling the metastatic spread of cancer. *Bull Math Biol* 81: 1965–2010. <https://doi.org/10.1007/s11538-019-00597-x>
5. Jiang WG, Sanders AJ, Katoh M, et al. (2015) Tissue invasion and metastasis: Molecular, biological and clinical perspectives. *Semin Cancer Biol* 35: S244–S275. <https://doi.org/10.1016/j.semcan.2015.03.008>
6. Meirson T and Gil-Henn H (2018) Targeting invadopodia for blocking breast cancer metastasis. *Drug Resist Update* 39: 1–17. <https://doi.org/10.1016/j.drup.2018.05.002>
7. Sibony-Benyamini H and Gil-Henn H (2012) Invadopodia: the leading force. *Eur J Cell Biol* 91: 896–901. <https://doi.org/10.1016/j.ejcb.2012.04.001>
8. Parekh A and Weaver AM (2016) Regulation of invadopodia by mechanical signaling. *Exp Cell Res* 343: 89–95. <https://doi.org/10.1016/j.yexcr.2015.10.038>
9. Deakin NE and Chaplain MAJ (2013) Mathematical modeling of cancer invasion: The role of membrane-bound matrix metalloproteinases. *Front Oncol* 3: 70. <https://doi.org/10.3389/fonc.2013.00070>
10. Chaplain M and Lolas (2006) Mathematical modelling of cancer invasion of tissue: dynamic heterogeneity. *Networks Heterog Media* 1: 399–439. <https://doi.org/10.3934/nhm.2006.1.399>
11. Ramis-Conde I, Chaplain MAJ, Anderson ARA (2008) Mathematical modelling of cancer cell invasion of tissue. *Math Comput Model* 47: 533–545. <https://doi.org/10.1016/j.mcm.2007.02.034>
12. Sfakianakis N, Madzvamuse A, Chaplain MAJ (2020) A hybrid multiscale model for cancer invasion of the extracellular matrix. *Multiscale Model Simul* 18: 824–850. <https://doi.org/10.1137/18M1189026>
13. Nska ZS, Rodrigo CM, Lachowicz M, et al. (2009) Tissue : the role and effect of nonlocal. *Math Model Methods Appl Sci* 19: 257–281. <https://doi.org/10.1142/S0218202509003425>
14. Saitou T, Rouzimaimaiti M, Koshikawa N, et al. (2012) Mathematical modeling of invadopodia formation. *J Theor Biol* 298: 138–146. <https://doi.org/10.1016/j.jtbi.2011.12.018>
15. Admon MA (2015) Mathematical modeling and simulation in an individual cancer cell associated with invadopodia formation [PhD Thesis]. Osaka University, Japan.
16. Gallinato O, Ohta M, Poignard C, et al. (2017) Free boundary problem for cell protrusion formations: theoretical and numerical aspects. *J Math Biol* 75: 263–307. <https://doi.org/10.1007/s00285-016-1080-7>

17. Admon MA and Suzuki T (2017) Signal transduction in the invadopodia formation using fixed domain method. *J Phys Conf Ser* 890: 012036. <https://doi.org/10.1088/1742-6596/890/1/012036>
18. Azhuan NAN, Poignard C, Suzuki T, et al. (2019) Two-dimensional signal transduction during the formation of invadopodia. *Malaysian J Math Sci* 13: 155–164.
19. Gallinato O, Colin T, Saut O, et al. (2017) Tumor growth model of ductal carcinoma: from in situ phase to stroma invasion. *J Theor Biol* 429: 253–266. <https://doi.org/10.1016/j.jtbi.2017.06.022>
20. Gallinato O and Poignard C (2017) Superconvergent second order Cartesian method for solving free boundary problem for invadopodia formation. *J Comput Phys* 339: 412–431. <https://doi.org/10.1016/j.jcp.2017.03.010>
21. Yaacob N, Noor Azhuan NA, Shafie S, et al. (2019) Numerical computation of signal stimulation from ligand-EGFR binding during invadopodia formation. *Matematika* 35: 139–148. <https://doi.org/10.11113/matematika.v35.n4.1268>
22. Osher S and Sethian JA (1988) Fronts propagating with curvature-dependent speed: Algorithms based on Hamilton-Jacobi formulations. *J Comput Phys* 79: 12–49. [https://doi.org/10.1016/0021-9991\(88\)90002-2](https://doi.org/10.1016/0021-9991(88)90002-2)
23. Sethian JA (1996) Theory, algorithms, and applications of level set methods for propagating interfaces. *Acta Numer* 5: 309–395. <https://doi.org/10.1017/S0962492900002671>
24. Chen S, Merriman B, Osher S, et al. (1997) A simple level set method for solving stefan problems. *J Comput Phys* 135: 8–29. <https://doi.org/10.1006/jcph.1997.5721>
25. Tan L and Zabaras N (2006) A level set simulation of dendritic solidification with combined features of front-tracking and fixed-domain methods. *J Comput Phys* 211: 36–63. <https://doi.org/10.1016/j.jcp.2005.05.013>
26. Tan L and Zabaras N (2007) A level set simulation of dendritic solidification of multi-component alloys. *J Comput Phys* 221: 9–40. <https://doi.org/10.1016/j.jcp.2006.06.003>
27. Tan L and Zabaras N (2007) Modeling the growth and interaction of multiple dendrites in solidification using a level set method. *J Comput Phys* 226: 131–55. <https://doi.org/10.1016/j.jcp.2007.03.023>
28. Sethian JA and Adalsteinsson D (1999) The fast construction of extension velocities in level set methods. *J Comput Phys* 148: 2–22. <https://doi.org/10.1006/jcph.1998.6090>
29. Shashni B, Ariyasu S, Takeda R, et al. (2018) Size-based differentiation of cancer and normal cells by a particle size analyzer assisted by a cell-recognition PC software. *Biol Pharm Bull* 41: 487–503. <https://doi.org/10.1248/bpb.b17-00776>
30. Li A, Dawson JC, Forero-Vargas M, et al. (2010) The actin-bundling protein fascin stabilizes actin in invadopodia and potentiates protrusive invasion. *Curr Biol* 20: 339–345. <https://doi.org/10.1016/j.cub.2009.12.035>
31. Oser M, Mader CC, Gil-Henn H, et al. (2010) Specific tyrosine phosphorylation sites on cortactin regulate Nck1-dependent actin polymerization in invadopodia. *J Cell Sci* 123: 3662–3673. <https://doi.org/10.1242/jcs.068163>
32. Ren XL, Qiao YD, Li JY, et al. (2018) Cortactin recruits FMNL2 to promote actin polymerization and endosome motility in invadopodia formation. *Cancer Lett* 419: 245–256. <https://doi.org/10.1016/j.canlet.2018.01.023>
33. Drummond ML, Li M, Tarapore E, et al. (2018) Actin polymerization controls cilia-mediated signaling. *J Cell Biol* 217: 3255–3266. <https://doi.org/10.1083/jcb.201703196>
34. Singh AB and Harris RC (2005) Autocrine, paracrine and juxtacrine signaling by EGFR ligands.

Cell Signal 17: 1183–1193. <https://doi.org/10.1016/j.cellsig.2005.03.026>

- 35. Walker D, Wood S, Southgate J, et al. (2006) An integrated agent-mathematical model of the effect of intercellular signalling via the epidermal growth factor receptor on cell proliferation. *J Theor Biol* 242: 774–789. <https://doi.org/10.1016/j.jtbi.2006.04.020>
- 36. Alroy I and Yarden Y (1997) The ErbB signaling network in embryogenesis and oncogenesis: Signal diversification through combinatorial ligand-receptor interactions. *FEBS Lett* 410: 83–86. [https://doi.org/10.1016/S0014-5793\(97\)00412-2](https://doi.org/10.1016/S0014-5793(97)00412-2)
- 37. Higashiyama S, Iwabuki H, Morimoto C, et al. (2008) Membrane-anchored growth factors, the epidermal growth factor family: beyond receptor ligands. *Cancer Sci* 99: 214–220. <https://doi.org/10.1111/j.1349-7006.2007.00676.x>
- 38. Hoshino D, Branch KM, Weaver AM (2013) Signaling inputs to invadopodia and podosomes. *J Cell Sci* 126: 2979–89. <https://doi.org/10.1242/jcs.079475>



AIMS Press

© 2022 the Author(s), licensee AIMS Press. This is an open access article distributed under the terms of the Creative Commons Attribution License (<http://creativecommons.org/licenses/by/4.0>)